The outgrowth of micrometastases is enabled by the formation of filopodium-like protrusions

Tsukasa Shibue[1,2], **Mary W. Brooks**[1,2], **M. Fatih Inan**[1,2], **Ferenc Reinhardt**[1,2], and **Robert A. Weinberg**[1,2,3]

[1]Whitehead Institute for Biomedical Research, Cambridge, Massachusetts

[2]MIT Ludwig Center for Molecular Oncology, Cambridge, Massachusetts

[3]Department of Biology, Massachusetts Institute of Technology, Cambridge, Massachusetts

Abstract

Disseminated cancer cells that have extravasated into the tissue parenchyma must interact productively with its extracellular matrix (ECM) components in order to survive, proliferate and form macroscopic metastases. The biochemical and cell-biological mechanisms enabling this interaction remain poorly understood. We find that the formation of elongated, integrin β_1-containing adhesion plaques by cancer cells that have extravasated into the lung parenchyma enables the proliferation of these cells via activation of focal adhesion kinase (FAK). These plaques originate in and appear only after the formation of filopodium-like protrusions (FLPs) that harbor integrin β_1 along their shafts. The cytoskeleton-regulating proteins Rif and mDia2 contribute critically to the formation of these protrusions and thereby enable the proliferation of extravasated cancer cells. Hence, the formation of FLPs represents a critical rate-limiting step for the subsequent development of macroscopic metastases.

Keywords

Metastatic colonization; Disseminated tumor cells; Cell-matrix adhesions; Actin cytoskeleton

Introduction

Hematogenous metastasis, the major cause of cancer-associated mortality, proceeds through the dissemination of cancer cells from the primary tumor via the circulation. The circulating cells eventually lodge in the capillary beds of distant organs, from which they may extravasate into the adjacent tissue parenchyma (1). The majority of extravasated cells either quickly undergo apoptosis or persist in the parenchyma of host tissue in a viable but non-proliferating state, and only rarely do they succeed in colonization, i.e., in generating macroscopic growths within such tissues (2, 3). The inability of cancer cells to survive and proliferate following extravasation appears to be attributable, in part, to the difficulties that these cells experience in adapting to the novel tissue microenvironments in which they have landed (4, 5). These microenvironments are likely defined by complex mixtures of growth factors, cytokines, and extracellular matrix (ECM) components (6).

Corresponding author: Robert A. Weinberg, Whitehead Institute for Biomedical Research, 9 Cambridge Center, Cambridge, MA 02142, phone: 1-617-258-5159, fax: 1-617-258-5230, weinberg@wi.mit.edu.

We and others have studied the behavior of cancer cells disseminated in the lung parenchyma using a set of three mouse mammary carcinoma cell lines – D2.0R, D2.1 and D2A1 – with differing potentials for metastasis (7–10). When introduced into mice via tail-vein injection, all three cell populations extravasate into the lung parenchyma with comparable efficiency and exhibit similar rates of initial survival (10). However, they show marked differences in subsequent proliferation and colony formation: the D2A1 cells proliferate rapidly after extravasation and colonize the lung tissue effectively, while the D2.0R and D2.1 cells fail to do so (10).

In the earlier studies, we and others undertook to model the post-extravasation behavior of the various D2 cell lines using an *in vitro* model system (9, 10). Thus, these cells were propagated in three-dimensional (3D) culture using the "Matrigel on-top (MoT)" method (11), in which cells are plated above a layer of undiluted Matrigel and then covered with Matrigel diluted 1:50 with culture medium. In our own case, these cells were prepared as single-cell suspensions and seeded at low densities (500–2000 cells/cm^2 bottom area; ref. 10). This ensured that individual cells were initially surrounded on all sides by ECM components, which modeled the conditions encountered by cancer cells immediately after extravasating into the lung parenchyma.

While these MoT conditions recapitulated only limited aspects of the *in vivo* microenvironment, they sufficed to reproduce the differing proliferation rates of the various D2 cell populations in the lungs. Thus, the D2A1 cells, which are far more aggressive *in vivo*, proliferated far more rapidly under MoT conditions than did the other two nonaggressive D2 cell types (9, 10). This contrasted with the behavior of these three cell types in monolayer culture, where they proliferated equally well (9, 10).

Subsequent analyses revealed that integrin-mediated interactions with the ECM proteins are essential for the aggressive D2A1 cells to proliferate rapidly both under MoT culture conditions and within the lung parenchyma (10). We also found that integrins containing the β$_1$ subunit contribute critically to these interactions, which confirmed previously reported observations by others (9, 12), and that these interactions ultimately enable rapid cell proliferation by triggering intracellular signaling events including the activation of focal adhesion kinase (FAK) (10).

In the present study, we identify the processes exploited by the recently extravasated, micrometastatic cancer cells in the lungs to establish productive interactions with the surrounding ECM. In brief, these processes begin with the formation of thin, actin-rich protrusions that harbor integrin β$_1$ together with other proteins that collaborate with integrins to form cell-matrix adhesions. These protrusions support the initial interactions between the extravasated cancer cells and ECM components of the lung parenchyma, thereby helping these cells to trigger adhesion-dependent signaling events including FAK activation. The resulting active FAK signaling, in turn, phosphorylates and activates extracellular signal-regulated kinases (ERKs) and thereby enables rapid proliferation of these cancer cells within the lung tissue.

Results

FAK/ERK signaling as a critical trigger for the post-extravasation proliferation

We undertook to elucidate the molecular basis for the differing proliferation rates of the various D2 cell populations, which were observed both when these cells were growing in MoT cultures and following their extravasation into the lung parenchyma (Supplementary Figs. S1A–E). This led us to discover the critical role of FAK-dependent activation of the ERKs – central mediators of various proliferation-promoting signals (13) – in determining

the proliferation rates under these conditions (ref. 10; Fig. 1A and Supplementary Figs. S2A–D).

Thus, FAK knockdown in the otherwise-aggressive D2A1 cells impaired their proliferation under MoT culture conditions, which was associated with a strong reduction in the phosphorylation of ERKs at residues critical to their activity (Fig. 1A). Working in the opposite direction, the ectopic expression of the constitutively-active CD2-FAK fusion protein in the otherwise-nonaggressive D2.0R and D2.1 cells elevated ERK phosphorylation levels and allowed these cells to proliferate rapidly under the MoT culture conditions (Supplementary Figs. S2A and S2B). Importantly, FAK signaling also contributed to ERK activation and thus to proliferation *in vivo* shortly after these cells had extravasated into the lung parenchyma (Figs. 1A, 1B and Supplementary Fig. S2D). In contrast, manipulation of FAK signaling did not discernibly affect either ERK phosphorylation levels or the proliferation rates when these various cell populations were growing as monolayers *in vitro* (Fig. 1A and Supplementary Figs. S2A–C).

We also found that the degree of the activation-associated phosphorylation of FAK and ERKs correlated closely with the abilities of the various populations of D2 cells to proliferate both under the MoT conditions of culture and within the lung parenchyma (ref. 10; Supplementary Figs. S3A–C). Taken together, these observations indicated that the activation status of FAK governed the activity of ERKs and thus critically determined the rate of cell proliferation under both conditions (Supplementary Fig. S3C). These observations prompted us to study the mechanisms that control FAK activation in cells growing under the MoT conditions of culture as well as in those that have extravasated into the lung parenchyma.

Assembly of elongated adhesion plaques as a controller of FAK signaling

We initially focused on the control of FAK phosphorylation in cells growing under *in vitro* MoT culture. Recruitment by ECM-ligated integrins is known to be crucial for the efficient phosphorylation and resulting activation of FAK (14). Moreover, we previously identified integrin β_1 as an integrin subunit essential for FAK activation in MoT-cultured D2A1 cells. Indeed, the knockdown of integrin β_1 expression in these cells diminished both autophosphorylation of FAK on its tyrosine residue 397 (Y397) and Src-mediated phosphorylation on tyrosine residue 861 (Y861) (10); both Y397 and Y861 are important phosphorylation sites for the FAK-dependent activation of multiple signaling events (14).

We also noted that the three D2 cell populations exhibited strikingly different patterns of integrin β_1 distribution under MoT culture conditions: in the majority of the aggressive D2A1 cells, abundant integrin β_1-containing, elongated adhesion plaques were assembled, while in the more indolent D2.0R and D2.1 cells, integrin β_1 was distributed evenly near the contact sites between Matrigel and the plasma membrane (ref. 10; Fig. 1C, Supplementary Figs. S4, S5A–C, S6A and S6B). The elongated morphology of adhesion plaques formed by the D2A1 cells is typical of the mature form of these plaques. Thus, earlier studies of fibroblasts growing in monolayer culture revealed that adhesions to ECM initially appear as small dots at the cell periphery, termed focal complexes. These dots are converted subsequently into ones having an oval-like or elongated morphology, which is often associated with the activation of a variety of signaling events (15).

We wished to determine whether the formation of these elongated adhesion plaques was accompanied by the activation of important signaling events, more specifically the phosphorylation of FAK, in the MoT-cultured D2A1 cells. In individual cells, we observed two distinct patterns of integrin β_1 accumulation: the majority of these cells displayed localization of integrin β_1 to elongated adhesion plaques, while the remaining cells exhibited

an even distribution of this integrin subunit near the plasma membrane ("peripheral accumulations"; Fig. 1D). We proceeded to measure the levels of FAK phosphorylation associated with each of these two patterns of integrin β_1 accumulation by immunostaining the cells for both integrin β_1 and phosphorylated FAK. This revealed that the ratio of pFAK-staining intensity to that of integrin β_1-staining was higher in the elongated plaques than in the peripheral accumulations, by 2.5 and 2.1 fold for pFAK [Y^{397}] and pFAK [Y^{861}], respectively (Fig. 1D). Hence, elongated plaque formation was correlated directly with elevated phosphorylation and thus activation of FAK.

In addition, within the population of MoT-cultured D2A1 cells, those cells that successfully assembled elongated, integrin β_1-containing adhesion plaques exhibited a 2.3-fold higher rate of Ki67 positivity – an indicator of proliferation – than did those that failed to form such plaques (Supplementary Fig. S5A). Hence, the development of such plaques and the associated more intense activation of FAK were correlated with and possibly critical to the rapid proliferation of D2A1 cells under MoT conditions.

We wished to extend these observations to understand the behavior of cells *in vivo* within the post-extravasation lung parenchyma. Thus, in order to analyze the formation of integrin β_1-containing, elongated adhesion plaques by the extravasated D2A1 cells, we used two different types of fluorescent fusion proteins: integrin α_5-YPet and α-actinin-Tag-RFP-T (Supplementary Fig. S7A; refs. 16, 17). Similarly constructed fluorescent marker proteins had been used successfully by others to monitor the localization of integrin α_5 and α-actinin in cells that were growing in monolayer culture (18).

Integrin α_5 associates exclusively with integrin β_1 to form heterodimeric integrin receptors, which are localized specifically to the elongated adhesion plaques in the MoT-cultured D2A1 cells (ref. 10; Supplementary Figs. S5B and S7B). Moreover, this integrin contributed critically to the proliferation of the D2A1 cells not only under the MoT culture conditions but also following the extravasation of these cells into the lung parenchyma (ref. 10; Supplementary Fig. S7C). These observations justified the use of integrin α_5-YPet to visualize integrin β_1-containing, elongated adhesion plaques by the D2A1 cells within the lung parenchyma. The actin-bundling α-actinin is one of the major components of the adhesion plaques formed in cells propagated under monolayer culture conditions as well as of those formed by the MoT-cultured D2A1 cells (ref. 19; Supplementary Fig. S5C). The combined use of these two fluorescent fusion proteins allowed us to verify that the observed plaques containing integrin α_5-YPet also recruited α-actinin and thus were functional.

Within the lung parenchyma, we found that the aggressive D2A1 cells formed abundant integrin α_5-YPet- and α-actinin-TagRFP-T-containing elongated adhesion plaques; these first became apparent 5 days after the intravenous injection of these cells. In contrast, echoing behavior observed in MoT cultures, plaques of this type were rarely formed by the more indolent D2.0R or D2.1 cells (Fig. 1C and Supplementary Fig. S4). Collectively, these various observations indicated that the abilities of various D2 cell populations to form elongated, mature adhesion plaques varied in concert with their abilities to activate FAK after extravasating into the lung parenchyma (Fig. 1C and Supplementary Fig. S3A). This suggested, in turn, that these elongated fusion plaques contribute functionally to the more potent activation of FAK in the aggressive D2A1 cells, which in turn facilitate ERK phosphorylation and thereby permit the rapid proliferation of these cells in the lung parenchyma.

Cytoskeletal protrusions that precede the appearance of elongated adhesion plaques

We undertook to uncover the mechanism(s) responsible for the differing abundance of integrin β_1-containing, elongated adhesion plaques among the various D2 cell populations

(Fig. 1C). To do so, we first studied the temporal development of these plaques in the MoT-cultured D2A1 cells by monitoring the localization of integrin β_1 together with that of actin cytoskeleton, whose dynamics is coupled tightly with the assembly of adhesion plaques (15).

Under the MoT culture conditions, the D2A1 cells began to exhibit integrin β_1-containing, elongated plaques earlier than they did so in the lung parenchyma: these plaques became apparent as early as 24 hours after starting the culture (Fig. 2A). We also found prominent protrusions displaying integrin β_1 that were colocalized with thin bundles of filamentous actin at this time (Figs. 2A–2C). These protrusions morphologically resembled filopodia – finger-like protrusions composed of parallel bundles of actin fibers; filopodium formation has been intensively studied in cells propagated as a monolayer (20, 21). These integrin β_1-containing, filopodium-like protrusions (hereafter referred to as FLPs) appeared as early as 6 hours after introducing the D2A1 cells into MoT culture (Fig. 2A).

In contrast to this behavior of the aggressive D2A1 cells, the metastasis-deficient D2.0R and D2.1 cells extended far fewer FLPs in MoT cultures (Fig. 2D and Supplementary Fig. S8A). Importantly, these differing abilities to form FLPs could also be observed in the lung tissue two days after the intravenous injection of these various D2 cell populations, where FLPs were visualized by a fluorescent actin marker lifeact-TagRFP-T (ref. 22; Fig. 2E and Supplementary Fig. S8A). These observations paralleled the differing abilities of these cell types to assemble integrin β_1-containing, elongated adhesion plaques that were observed both under MoT culture conditions and in the lung parenchyma (Fig. 1C). Together, these correlations prompted us to hypothesize that the formation of FLPs and the assembly of elongated adhesion plaques are functionally interrelated in cells growing under both conditions.

We then explored whether other types of metastasis-competent cells also form FLPs and elongated adhesion plaques resembling those observed in the aggressive D2A1 cells. Thus, we examined various human breast cancer cell lines that show differing metastatic powers upon implantation into mice. Twelve hours after being cultured under MoT conditions, 7 out of the 9 types of metastatic cells, but none of the 9 types of nonmetastatic cells, exhibited one or more FLP per cell (Fig. 3A). Moreover, after 5 days of MoT culture, 7 out of 9 metastatic cells, but none of the 9 nonmetastatic cells, exhibited a significant proportion of cells (> 5% of cell population) that had developed integrin β_1-containing, elongated adhesion plaques (Fig. 3B). Hence, under *in vitro* MoT culture conditions, a variety of metastasis-competent cells developed both FLPs and elongated adhesion plaques far more frequently than did the metastasis-deficient cells.

In addition, following extravasation into the lung parenchyma *in vivo*, the metastasis-competent breast cancer cell lines Sum159, BT549, MDA-MB-231 and Sum1315 developed far more abundant FLPs (> 3.6-fold increase in FLP number per cell on average) and assembled elongated adhesion plaques far more frequently (by > 30-fold larger proportion of cell populations on average) than did the metastasis-deficient SKBR3 and ZR-75-1 cells (Figs. 3C, 3D, Supplementary Figs. S8B and S8C). These extensive correlations between metastasis competence on the one hand, and the ability to form FLPs and elongated adhesion plaques on the other, provided additional confirmation of the notion that the formation of these structures provides critical support for the subsequent development of macroscopic metastases. However, it still remained unclear whether and how the formation of FLPs contributes to the subsequent assembly of elongated adhesion plaques.

Functional connection between FLP formation and adhesion plaque assembly

The model proposed here – that FLPs are involved in the formation of elongated, mature adhesion plaques – contrasted with the widely accepted view of the process of mature adhesion plaque formation in cells that are propagated as monolayers *in vitro*. Thus, the majority of mature adhesion plaques in monolayer-cultured cells are thought to be formed independently of filopodia, i.e., the actin-rich protrusions that morphologically resemble FLPs. Indeed, these adhesion plaques have been found to originate largely from dot-like focal complexes formed beneath lamellipodia – sheet-like protrusions that are morphologically and functionally distinct from filopodia (15) – in monolayer-cultured cells.

Importantly, lamellipodial protrusions were rarely observed when cells were propagated within the 3D gels (23), although the formation of elongated, mature adhesion plaques were repeatedly observed in various cell types propagated within such gels (reviewed in ref. 24). These observations by others, together with our present observations of FLPs, led us to speculate that certain types of 3D-cultured cells employ an FLP-mediated mechanism of mature adhesion plaque formation instead of relying on the lamellipodium-dependent mechanism.

In order to elucidate the connection between FLPs and elongated adhesion plaques, we asked whether FLPs interact with the proteins involved in cell-ECM adhesions in a way different from filopodia formed by monolayer-cultured cells (Figs. 4A–4C, Supplementary Figs. S9A–D, Supplementary Movies S1 and S2). We found that integrin β_1 was distributed along the length of the shafts of FLPs in the MoT-cultured D2A1 cells (Fig. 4A). In contrast, confirming previous observations by others (25, 26), integrin β_1 was enriched at the tips of filopodia in the D2A1 cells growing as a monolayer (Fig. 4A). These observations were consistent with the notion that FLPs contribute to the formation of integrin-mediated adhesions in a manner different from filopodia.

We proceeded to analyze the association with FLPs of major adhesion plaque proteins — FAK, talin1 and paxillin. We found that these adhesion plaque proteins were recruited progressively to FLPs in the MoT-cultured D2A1 cells (Fig. 4D, Supplementary Figs. S10A and S10B). These results, together with the temporal order of FLP formation prior to the assembly of elongated adhesion plaques (Fig. 2A), indicated that the protein components of these plaques, including integrin subunits (e.g., β_1) and adhesion plaque proteins (e.g., FAK, talin1 and paxillin), first accumulate in FLPs prior to their association with elongated adhesion plaques.

To directly observe the relationship between FLP formation and elongated adhesion plaque assembly, we performed time-lapse microscopy analyses on the integrin α_5-YPet-expressing D2A1 cells growing in MoT culture. We found that among a group of 235 cells that did not display elongated adhesion plaques at the beginning of observation, 129 (55%) cells exhibited the formation of FLPs either at the beginning or during the course of the observation period, while the remaining 106 (45%) cells never developed FLPs (Fig. 4E). Notably, 61 out of the 129 FLP-forming cells, but none of the 106 FLP-non-forming cells, eventually developed elongated adhesion plaques.

This correlation strongly suggested that FLP formation is a prerequisite for the development of elongated adhesion plaques in these cells. Moreover, with increasing time, we observed the progressive centripetal movement of the FLP-associated integrin α_5-YPet complexes (0–80 min; Fig. 4F and Supplementary Movie S3). This ultimately resulted in the translocation of these complexes into elongated adhesion plaques that were aligned with the cell surface (140–160 min; Fig. 4F and Supplementary Movie S3). Hence, the cluster of integrins displayed along the lengths of FLPs, presumably together with associated adhesion plaque

proteins, served as precursors of those that accumulate in elongated, mature adhesion plaques. Collectively, these observations prompted us to postulate that FLPs contribute to the assembly of mature adhesion plaques by fostering the nucleation of protein complexes that comprise the core of these plaques.

Rif/mDia2 signaling in FLP formation and metastatic colonization

The findings described above demonstrated that the rapid proliferation of cancer cells under MoT culture conditions *in vitro* and within the lung parenchyma *in vivo* is preceded by a series of changes that are initiated by the formation of FLPs. Thus, under these conditions, FLP formation appeared to contribute critically to the assembly of elongated, mature adhesion plaques, which in turn triggers FAK/ERK signaling and thereby ultimately permits rapid cell proliferation.

In order to confirm the causal contribution of these initial steps, we undertook to test the effects of blocking FLP formation. A number of proteins, notably Cdc42, fascin1, Rif, mDia2, IRSp53, myosin X and Ena/VASP, have been associated with the formation of filopodia in monolayer-cultured cells (21); the last of these subsumes a group of three actin-binding proteins – Mena, VASP and Evl (27). Based on the structural similarity between filopodia and FLPs (Figs. 4A and 4B), we speculated that some of these regulators of filopodia also contribute to the formation of FLPs in cells growing under MoT culture conditions. Accordingly, we proceeded to examine the involvement of these proteins in FLP formation.

We found that the knockdown of Cdc42, Rif, mDia2 or myosin X expression, as well as the functional inhibition of Ena/VASP proteins by the VASP-TD fragment – a dominant-negative inhibitor for all three Ena/VASP proteins (28) –, both resulted in significant (42–61%) decreases in the number of FLPs formed by MoT-cultured D2A1 cells. These decreases in FLP number were associated with 42–90% reductions in cell number when these cells were propagated for 10 days under MoT conditions, whereas none of these manipulations caused more than 13% decrease in cell number when these cells were propagated as monolayers for the same period of time (Figs. 5A, 5B and Supplementary Figs. S11A–F). In contrast, knocking down the expression of either fascin1 or IRSp53, neither of which participated in FLP formation in the D2A1 cells growing under the MoT conditions (Fig. 5A), failed to discernibly affect the proliferation of these cells under these conditions (Fig. 5B). Based on these extensive correlations, we concluded that in the MoT-cultured D2A1 cells, the formation of FLPs contributes critically to the ability of these cells to proliferate rapidly.

Among the proteins that were involved in FLP formation in the D2A1 cells, Rif and mDia2 were of particular interest for the following reasons: First, in certain types of monolayer-cultured cells, the driving force of filopodial protrusion is provided by the mDia2-mediated actin nucleation and polymerization, which in turn can be activated by a Rho-family GTPase Rif; this suggested the central role of Rif/mDia2 signaling in the formation of certain types of filopodia and similar protrusions (29). Second, in the D2A1 cells growing under MoT conditions, the knockdown of either Rif or mDia2 expression had a more potent effect than did the knockdown of the other filopodium-regulators tested here on both FLP formation and proliferation (see Figs. 5A and 5B). Third, Rif was found to be localized along the shafts of FLPs formed in the MoT-cultured D2A1 cells, while mDia2 was enriched at their tips; this reflected the distribution patterns of Rif and mDia2 within filopodia extending from HeLa cells propagated as a monolayer (Fig. 5C; ref. 30). Collectively, these observations suggested the importance of Rif/mDia2 signaling in enabling the abundant display of FLPs in the MoT-cultured D2A1 cells.

These considerations prompted us to analyze in detail the effect of Rif or mDia2 knockdown on the behavior of the D2A1 cells growing under MoT culture conditions. We found that the development by these cells of integrin β_1-containing, elongated adhesion plaques, as well as the activation of FAK and ERKs, was significantly impaired by the knockdown of Rif or mDia2 expression (Figs. 5D and 5E). In contrast, neither of these knockdowns noticeably affected the activation status of FAK and ERKs when the D2A1 cells were growing as a monolayer (Fig. 5E). Moreover, the reduced proliferation under MoT culture conditions of both Rif-knockdown and mDia2-knockdown D2A1 cells was reversed by the concomitant expression of the constitutively active CD2-FAK in these cells (Fig. 5F and Supplementary Fig. S11C). Hence, Rif/mDia2-dependent formation of FLPs in cells propagated under MoT culture conditions contributes to the proliferation of these cells largely, if not entirely, by promoting the assembly of integrin β_1-containing, elongated adhesion plaques, thereby facilitating FAK activation.

We also examined the role of Rif/mDia2 signaling in the behavior of the D2A1 cells disseminated within the lungs. The efficiency of extravasation into the lung parenchyma was not noticeably affected by the knockdown of Rif or mDia2 expression (Supplementary Figs. S12A and S12B). However, both the Rif-knockdown and mDia2-knockdown cells exhibited significantly reduced (48–57%) numbers of FLPs compared to the control cells shortly after these cells had infiltrated into the lung parenchyma (Fig. 6A). This was associated with impaired development of elongated adhesion plaques, reduced levels of FAK phosphorylation on Y397 and Y861, as well as decreased proliferation rates (Figs. 6B–6D). These observations indicated a functional connection between Rif/mDia2-dependent FLP formation and proliferation in the D2A1 cells that had extravasated into the lung parenchyma. Importantly, Rif-knockdown and mDia2-knockdown cells ultimately developed 8.2 to 13.2 fold reduced numbers of macroscopic metastases in the lungs relative to the control D2A1 cells injected in parallel, as examined 24 days after the injection (Fig. 6D).

We also examined in detail the lung sections that were harvested 10 days after the injection. Here again, the knockdown of Rif or mDia2 expression in the D2A1 cells decreased (2.5 to 3.9 fold) the numbers of macroscopic metastases (> 20 cells/colony) that were observed in these sections (Fig. 6E). Interestingly, however, the numbers of microscopic metastases (20 cells/colony), which were composed mostly (> 90%) of viable but nonproliferating cells (Supplementary Fig. S13A), were actually increased (1.7 to 2.3 fold) by these knockdowns (Fig. 6E). Collectively, these observations indicated that the knockdown of Rif or mDia2 expression diminishes the ability of the otherwise-aggressive D2A1 cells to proliferate rapidly following extravasation into the lung parenchyma, thereby forcing these cells to remain quiescent in the lung tissue without apparently dying or proliferating.

The inhibitory effect of Rif or mDia2 knockdown on macroscopic lung metastasis formation was also observed following the tail-vein injection of TS/A mouse mammary carcinoma cells (Supplementary Figs. S11D–S11F and S13B), while these knockdowns did not discernibly affect the proliferation of these cells in monolayer culture (Supplementary Fig. S11F). Hence, multiple metastasis-competent cell types rely on Rif/mDia2 signaling for efficiently colonizing the lung tissue. We also found that the ability of Rif-knockdown and mDia2-knockdown D2A1 cells to form macroscopic lung metastases could be partially restored by ectopically expressing the constitutively active CD2-FAK fusion protein in these cells (Fig. 6F). This supported the role of FAK as a key signaling mediator connecting Rif/mDia2-dependent FLP formation and the development of macroscopic metastases (Fig. 7A).

We proceeded to further substantiate the causal connection between the formation of FLPs and proliferation by extravasated cancer cells. To do so, we tested the effects of other

strategies that simultaneously blocked FLP formation and proliferation in the D2A1 cells growing under the MoT conditions of culture: these included the knockdown of Cdc42 expression as well as the expression of dominant-negative constructs for the Cdc42 (Cdc42 T17N; ref. 31) or Ena/VASP proteins (VASP-TD) (Figs. 5A, 5B, Supplementary Figs. S14A-D). Here again, we observed that all three manipulations concomitantly impaired the FLP-forming ability and proliferation potential of the D2A1 cells that were infiltrated into the lung parenchyma following tail-vein injection (Figs. 6A, 6D and Supplementary Figs. S15A–E). Moreover, these manipulated cells ultimately developed 57–72% fewer numbers of macroscopic lung metastases than did the control cells injected in parallel (Fig. 6D and Supplementary Fig. S15D), while none of these manipulations noticeably affected the proliferation of the D2A1 cells in monolayer culture (Fig. 5B and Supplementary Fig. S14C)

In contrast, the knockdown of the expression of fascin1, an actin-bundling protein dispensable for the formation of FLPs under MoT conditions, also failed to block FLP formation by the extravasated D2A1 cells in the lung parenchyma (Figs. 5A and 6A). Moreover, fascin1 knockdown did not noticeably inhibit the proliferation of the D2A1 cells within the lung tissue (Fig. 6D and Supplementary Fig. S15F). These observations lent further support to the model that the formation of FLPs by disseminated cancer cells contributes critically to metastatic colonization.

We also asked whether the enforced activation of Rif or mDia2 in the otherwise-nonaggressive D2.0R and D2.1 cells enabled them to extend abundant FLPs, thereby ultimately allowing these cells to proliferate rapidly under MoT culture conditions *in vitro* and within the lung parenchyma *in vivo* (Supplementary Figs. S16A–E and S17A). As expected, the ectopic expression of the constitutively active mutant of Rif or mDia2 (Rif Q77L and mDia2 M1041A) enabled the D2.0R and D2.1 cells to form abundant actin-rich protrusions under MoT conditions of culture, which were morphologically indistinguishable from FLPs formed naturally by the aggressive D2A1 cells (Supplementary Fig. S16A). However, these manipulated D2.0R and D2.1 cells subsequently failed to develop abundant, elongated adhesion plaques containing integrin β_1 and they exhibited only modest, if any, increases in the rate of proliferation under MoT culture conditions relative to the respective control cells (Supplementary Figs. S16 C and S16D). Moreover, the expression of Rif Q77L and mDia2 M1041A did not noticeably enhance the ability of the D2.0R and D2.1 cells to form macroscopic lung metastases following tail-vein injection (Supplementary Fig. S17A). Collectively, these observations indicated that the formation of FLPs is necessary, but not sufficient to enable the rapid proliferation of cancer cells under MoT culture conditions *in vitro* and within the lung parenchyma *in vivo*.

The role of Rif/mDia2 signaling in tumor progression

We proceeded to determine whether the proteins that were involved in the formation of FLPs also contributed to primary tumor formation. Accordingly, we implanted Rif-knockdown and mDia2-knockdown D2A1 cells orthotopically in mouse mammary fat pads. We observed that the sizes of the resulting primary tumors were not noticeably affected by these knockdowns (Fig. 7B). Moreover, the control, Rif-knockdown and mDia2-knockdown D2A1 cells exhibited comparable rates of proliferation within these established tumors (Fig. 7B).

We also examined the effects of Rif knockdown on the spontaneous metastasis from the orthotopically implanted tumors generated by TS/A cells, which usually spawn large numbers of metastases in both the lungs and liver. As was the case with D2A1 cells, the orthotopically-implanted control and Rif-knockdown TS/A cells yielded primary tumors of similar sizes, within which these cells exhibited comparable proliferation rates regardless of the knockdown of Rif expression (Fig. 7C and Supplementary Fig. S17B). In contrast, Rif

knockdown led to substantially decreased numbers of macrometastases spawned by the TS/A primary tumors, not only in the lungs (81–92% decrease) but also in the liver (87–100%) (Fig. 7C and Supplementary Fig. S17B).

These observations pointed to a profound difference in the mechanisms governing the proliferation of cancer cells within already-established primary tumors and shortly after extravasating into the parenchyma of foreign tissues. Thus, the Rif- and mDia2-dependent mechanism of FLP formation is dispensable for the proliferation of cancer cells within the established primary tumors. However, it represents an important mechanism employed by cancer cells to enable their proliferation soon after these cells directly confront the ECM environment within the foreign tissue parenchyma, specifically those of the lungs and liver (Fig. 7A).

We extended these findings by inhibiting FLP formation in B16F10 mouse melanoma cells (32), which efficiently generate macroscopic metastases in various organs following intracardiac injection (33). We found that macrometastasis formations by the intracardially-injected B16F10 melanoma cells in the lungs, liver and bone marrow, were all significantly impaired by the knockdown of Rif expression in these cells (Fig. 7D). In contrast, the growth of primary tumors following subcutaneous implantation of the B16F10 cells were not noticeably affected by this knockdown (Supplementary Fig. S17C). These results supported the notion that Rif, and presumably other proteins involved in the formation of FLPs, contribute in critical ways to the establishment of macroscopic metastases in multiple target organs.

Discussion

Systemic dissemination of cancer cells is frequently observed in both breast and prostate cancer patients. However, the numbers of disseminated cells clearly dwarf those of successfully formed metastases (34), provoking the question of why metastatic colonization is so inefficient. Clearly, enormous attrition of cancer cells occurs in the interval between the lodging of disseminated cells in microvessels and the establishment of macroscopic metastases (35).

We postulate that at least three impediments obstruct the path toward successful metastasis formation. First, cancer cells must enter the parenchyma of a foreign tissue, either by invading through capillaries walls or by proliferating intraluminally and then rupturing the endothelium. Second, they must survive and initiate proliferation by establishing productive connections with the parenchymal ECM. Third, they must adapt to unfamiliar growth factor and cytokine environments in order to acquire mitogenic and trophic signals (36). Here we have studied the second of these processes – how disseminated cells initiate proliferation after confronting the ECM environment of a foreign tissue parenchyma.

The findings presented here collectively prompt us to propose that in certain and perhaps many types of metastatic cells, the chain of processes governing the initial proliferation of cancer cells within the post-extravasation tissue parenchyma can be depicted as follows: formation of filopodium-like protrusions (FLPs) containing integrin β_1 along the length of their shafts → recruitment of adhesion plaque proteins to these integrin β_1-containing FLPs → assembly of elongated, mature adhesion plaques following the centripetal movement of integrin clusters → FAK activation within these mature adhesion plaques → FAK-dependent activation of ERKs → cell proliferation (Fig. 7A).

The FLPs that enabled the rapid proliferation of extravasated cancer cells morphologically resemble filopodia extended by monolayer-cultured cells: both are actin-rich protrusions exhibiting finger-like shapes. However, there are also important distinctions between

filopodia and FLPs. Thus, while integrin β_1 is enriched at the tips of filopodia, this integrin subunit was found to be distributed evenly along the shafts of FLPs (Fig. 4A). In addition, we observed a profound difference in the lifetime of these two types of protrusions: while the 80% of filopodia retracted within 30 minutes after initial extension, the majority (> 90%) of FLPs survived longer than 60 minutes (Fig. 4C, Supplementary Movies S1 and S2). The detailed relationship of FLPs to the filopodia formed by monolayer-cultured cells awaits future study.

The set of cytoskeleton regulatory proteins involved in the formation of FLPs following extravasation overlaps partially with those that regulate invasiveness, an attribute essential for completing an earlier step of the invasion-metastasis cascade (37). Thus, Cdc42 and mDia2, two important regulators of FLP formation (Fig. 5A), are also involved in fibroblast invasion through collagen matrices and kidney epithelial cell migration, respectively (38, 39). However, we also found considerable differences between the mechanism controlling invasiveness and the one regulating FLP formation. Thus, the knockdown of Rif expression, which efficiently blocks the formation of FLPs by the D2A1 cells within the lung parenchyma, did not noticeably affect their invasiveness through the Boyden chamber (data not shown). Moreover, FLPs formed under MoT culture conditions are organized differently from invadopodia – protrusions that are formed by cells propagated above a film of ECM and are thought to contribute to cancer cell invasiveness (Supplementary Fig. S9B; ref. 40). This reinforces the notion that cancer cells employ distinct sets of actin-regulating proteins in executing the different steps of the invasion-metastasis cascade.

By studying further the role of the protein regulators of FLP formation in controlling cancer cell behaviors, we found that these proteins were dispensable for the continuous proliferation of cancer cells within already-established primary tumors (Fig. 7B and Supplementary Fig. S17B). This would suggest, in turn, that during the progression of primary tumors, the acquired ability to extend abundant FLPs is unlikely to be selectively advantageous to the cells within these tumors. Moreover, as described above, cancer cell invasion from the primary tumors appears to be governed by a set of actin-regulating proteins distinct from those enabling abundant FLP formation. Collectively, these observations might provide an explanation for the inability of the majority of cancer cells to initiate proliferation after leaving the primary site and infiltrating into the parenchyma of foreign tissues, where the ability of FLP formation is indeed critical to the initiation of proliferation.

The present study leaves several significant issues unresolved. These include the molecular determinants of the differing abundance of FLPs among the various populations of the D2 cells. In addition, we also found a reduced incidence of primary tumors following the orthotopic implantation of cells that have been manipulated to block the formation of FLPs. Thus, manipulations that block FLP formation, including the knockdown of either Rif or mDia2 expression, as well as the overexpression of the dominant-negative Cdc42 T17N, all significantly reduced the incidence of primary tumors by orthotopically-implanted D2A1 cells (12 to 1400 fold decreases in the estimated frequency of tumor-initiating cells; data not shown). This suggests, but does not prove, that the molecular machinery governing the formation of FLPs in the micrometastatic cancer cells also contributes critically to the initial establishment of primary tumors after orthotopic implantation of certain types of cancer cells. These issues will be addressed in a subsequent study.

Methods

Plasmids

The lentiviral vectors expressing protein-coding DNA sequences used in this study were generated using pLV-IRES-neo (10), pLV-IRES-puro or pLV-IRES-EGFP as a backbone. pLKO-puro was used as backbones for the lentiviral vectors expressing short hairpin RNAs (shRNAs).

Cell culture

Mouse mammary carcinoma D2 cell lines (D2.0R, D2.1 and D2A1) and TS/A cell line were gifts from FR Miller and PL Lollini, respectively (7, 41). Human mammary carcinoma cell lines MCF10A, Sum1315, Sum149 and Sum159 were gifts from SP Ethier (42, 43). All these cells were maintained as described previously (10, 41, 44). Human mammary carcinoma cell lines BT474, BT549, MCF7, MDA-MB-157, -231, -436, -453, -468, SK-BR-3, T47D and ZR-75-1, as well as mouse melanoma cell line B16F10, were obtained from ATCC and maintained according to the provider's protocol. The preparation and maintenance of human mammary epithelial cell lines HME, HMLER and BPLER were described previously (45, 46). The human mammary carcinoma cell lines MCF10A, Sum149, Sum159, BT474, BT549, MCF7, MDA-MB-157, -231, -453, -468, SK-BR-3 and T47D, as well as the human mammary epithelial cell lines used here, were authenticated by microarray analysis. The other human mammary carcinoma cell lines, as well as the mouse cell lines used here, were not passaged more than 6 months after receipt.

Statistical Analysis

Statistical analyses were carried out by Student's *t*-test, unless otherwise indicated.

Supplementary Material

Refer to Web version on PubMed Central for supplementary material.

Acknowledgments

References

1. Fidler IJ. The pathogenesis of cancer metastasis: the 'seed and soil' hypothesis revisited. Nat Rev Cancer. 2003; 3:453–8. [PubMed: 12778135]

2. Mareel, MM.; De Baetselier, P.; Roy, MV. Mechanism of Invasion and Metastasis. 1. Boca Raton: CRC press; 1991.

3. Hedley BD, Chambers AF. Tumor dormancy and metastasis. Adv Cancer Res. 2009; 102:67–101. [PubMed: 19595307]

4. Barkan D, Green JE, Chambers AF. Extracellular matrix: a gatekeeper in the transition from dormancy to metastatic growth. Eur J Cancer. 2010; 46:1181–8. [PubMed: 20304630]

5. Shibue T, Weinberg RA. Metastatic colonization: Settlement, adaptation and propagation of tumor cells in a foreign tissue environment. Semin Cancer Biol. 2011; 21:99–106. [PubMed: 21145969]

6. Joyce JA, Pollard JW. Microenvironmental regulation of metastasis. Nat Rev Cancer. 2009; 9:239–52. [PubMed: 19279573]

7. Rak JW, McEachern D, Miller FR. Sequential alteration of peanut agglutinin binding-glycoprotein expression during progression of murine mammary neoplasia. Br J Cancer. 1992; 65:641–8. [PubMed: 1586590]

8. Morris VL, Koop S, MacDonald IC, et al. Mammary carcinoma cell lines of high and low metastatic potential differ not in extravasation but in subsequent migration and growth. Clin Exp Metastasis. 1994; 12:357–67. [PubMed: 7923988]

9. Barkan D, Kleinman H, Simmons JL, et al. Inhibition of metastatic outgrowth from single dormant tumor cells by targeting the cytoskeleton. Cancer Res. 2008; 68:6241–50. [PubMed: 18676848]

10. Shibue T, Weinberg RA. Integrin beta1-focal adhesion kinase signaling directs the proliferation of metastatic cancer cells disseminated in the lungs. Proc Natl Acad Sci U S A. 2009; 106:10290–5. [PubMed: 19502425]

11. Debnath J, Brugge JS. Modelling glandular epithelial cancers in three-dimensional cultures. Nat Rev Cancer. 2005; 5:675–88. [PubMed: 16148884]

12. Weaver VM, Petersen OW, Wang F, et al. Reversion of the malignant phenotype of human breast cells in three-dimensional culture and in vivo by integrin blocking antibodies. J Cell Biol. 1997; 137:231–45. [PubMed: 9105051]

13. Roberts PJ, Der CJ. Targeting the Raf-MEK-ERK mitogen-activated protein kinase cascade for the treatment of cancer. Oncogene. 2007; 26:3291–310. [PubMed: 17496923]

14. Tilghman RW, Parsons JT. Focal adhesion kinase as a regulator of cell tension in the progression of cancer. Semin Cancer Biol. 2008; 18:45–52. [PubMed: 17928235]

15. Geiger B, Bershadsky A, Pankov R, Yamada KM. Transmembrane crosstalk between the extracellular matrix--cytoskeleton crosstalk. Nat Rev Mol Cell Biol. 2001; 2:793–805. [PubMed: 11715046]

16. Nguyen AW, Daugherty PS. Evolutionary optimization of fluorescent proteins for intracellular FRET. Nat Biotechnol. 2005; 23:355–60. [PubMed: 15696158]

17. Shaner NC, Lin MZ, McKeown MR, et al. Improving the photostability of bright monomeric orange and red fluorescent proteins. Nat Methods. 2008; 5:545–51. [PubMed: 18454154]

18. Laukaitis CM, Webb DJ, Donais K, Horwitz AF. Differential dynamics of alpha 5 integrin, paxillin, and alpha-actinin during formation and disassembly of adhesions in migrating cells. J Cell Biol. 2001; 153:1427–40. [PubMed: 11425873]

19. Zaidel-Bar R, Ballestrem C, Kam Z, Geiger B. Early molecular events in the assembly of matrix adhesions at the leading edge of migrating cells. J Cell Sci. 2003; 116:4605–13. [PubMed: 14576354]

20. Gupton SL, Gertler FB. Filopodia: the fingers that do the walking. Sci STKE. 2007; 2007:re5. [PubMed: 17712139]

21. Mattila PK, Lappalainen P. Filopodia: molecular architecture and cellular functions. Nat Rev Mol Cell Biol. 2008; 9:446–54. [PubMed: 18464790]

22. Riedl J, Crevenna AH, Kessenbrock K, et al. Lifeact: a versatile marker to visualize F-actin. Nat Methods. 2008; 5:605–7. [PubMed: 18536722]

23. Beningo KA, Dembo M, Wang YL. Responses of fibroblasts to anchorage of dorsal extracellular matrix receptors. Proc Natl Acad Sci U S A. 2004; 101:18024–9. [PubMed: 15601776]

24. Harunaga JS, Yamada KM. Cell-matrix adhesions in 3D. Matrix Biol. 2011; 30:363–8. [PubMed: 21723391]

25. Grabham PW, Goldberg DJ. Nerve growth factor stimulates the accumulation of beta1 integrin at the tips of filopodia in the growth cones of sympathetic neurons. J Neurosci. 1997; 17:5455–65. [PubMed: 9204928]

26. Galbraith CG, Yamada KM, Galbraith JA. Polymerizing actin fibers position integrins primed to probe for adhesion sites. Science. 2007; 315:992–5. [PubMed: 17303755]

27. Bear JE, Gertler FB. Ena/VASP: towards resolving a pointed controversy at the barbed end. J Cell Sci. 2009; 122:1947–53. [PubMed: 19494122]

28. Vasioukhin V, Bauer C, Yin M, Fuchs E. Directed actin polymerization is the driving force for epithelial cell-cell adhesion. Cell. 2000; 100:209–19. [PubMed: 10660044]

29. DeWard AD, Eisenmann KM, Matheson SF, Alberts AS. The role of formins in human disease. Biochim Biophys Acta. 2010; 1803:226–33. [PubMed: 19941910]

30. Pellegrin S, Mellor H. The Rho family GTPase Rif induces filopodia through mDia2. Curr Biol. 2005; 15:129–33. [PubMed: 15668168]

31. Nobes CD, Hall A. Rho, rac, and cdc42 GTPases regulate the assembly of multimolecular focal complexes associated with actin stress fibers, lamellipodia, and filopodia. Cell. 1995; 81:53–62. [PubMed: 7536630]

32. Fidler IJ. Selection of successive tumour lines for metastasis. Nat New Biol. 1973; 242:148–9. [PubMed: 4512654]

33. Arguello F, Baggs RB, Frantz CN. A murine model of experimental metastasis to bone and bone marrow. Cancer Res. 1988; 48:6876–81. [PubMed: 3180096]

34. Riethmuller G, Klein CA. Early cancer cell dissemination and late metastatic relapse: clinical reflections and biological approaches to the dormancy problem in patients. Semin Cancer Biol. 2001; 11:307–11. [PubMed: 11513566]

35. Chambers AF, Groom AC, MacDonald IC. Dissemination and growth of cancer cells in metastatic sites. Nat Rev Cancer. 2002; 2:563–72. [PubMed: 12154349]

36. Nguyen DX, Bos PD, Massague J. Metastasis: from dissemination to organ-specific colonization. Nat Rev Cancer. 2009; 9:274–84. [PubMed: 19308067]

37. Nurnberg A, Kitzing T, Grosse R. Nucleating actin for invasion. Nat Rev Cancer. 2011; 11:177–87. [PubMed: 21326322]

38. Banyard J, Anand-Apte B, Symons M, Zetter BR. Motility and invasion are differentially modulated by Rho family GTPases. Oncogene. 2000; 19:580–91. [PubMed: 10698528]

39. Gupton SL, Eisenmann K, Alberts AS, Waterman-Storer CM. mDia2 regulates actin and focal adhesion dynamics and organization in the lamella for efficient epithelial cell migration. J Cell Sci. 2007; 120:3475–87. [PubMed: 17855386]

40. Buccione R, Caldieri G, Ayala I. Invadopodia: specialized tumor cell structures for the focal degradation of the extracellular matrix. Cancer Metastasis Rev. 2009; 28:137–49. [PubMed: 19153671]

41. Nanni P, de Giovanni C, Lollini PL, Nicoletti G, Prodi G. TS/A: a new metastasizing cell line from a BALB/c spontaneous mammary adenocarcinoma. Clin Exp Metastasis. 1983; 1:373–80. [PubMed: 6546207]

42. Soule HD, Maloney TM, Wolman SR, et al. Isolation and characterization of a spontaneously immortalized human breast epithelial cell line, MCF-10. Cancer Res. 1990; 50:6075–86. [PubMed: 1975513]

43. Ignatoski KM, Ethier SP. Constitutive activation of pp125fak in newly isolated human breast cancer cell lines. Breast Cancer Res Treat. 1999; 54:173–82. [PubMed: 10424408]

44. Kuperwasser C, Dessain S, Bierbaum BE, et al. A mouse model of human breast cancer metastasis to human bone. Cancer Res. 2005; 65:6130–8. [PubMed: 16024614]

45. Elenbaas B, Spirio L, Koerner F, et al. Human breast cancer cells generated by oncogenic transformation of primary mammary epithelial cells. Genes Dev. 2001; 15:50–65. [PubMed: 11156605]

46. Ince TA, Richardson AL, Bell GW, et al. Transformation of different human breast epithelial cell types leads to distinct tumor phenotypes. Cancer Cell. 2007; 12:160–70. [PubMed: 17692807]

Significance

While the mechanisms of metastatic dissemination have begun to be uncovered, those involved in the establishment of extravasated cancer cells in foreign tissue microenvironments remained largely obscure. We have studied the behavior of recently extravasated cancer cells in the lungs and identified a series of cell-biological processes, involving the formation of filopodium-like protrusions (FLPs) and the subsequent development of elongated, mature adhesion plaques, which contribute critically to the rapid proliferation of the micrometastatic cells and thus are prerequisites to the eventual lung colonization by these cells.
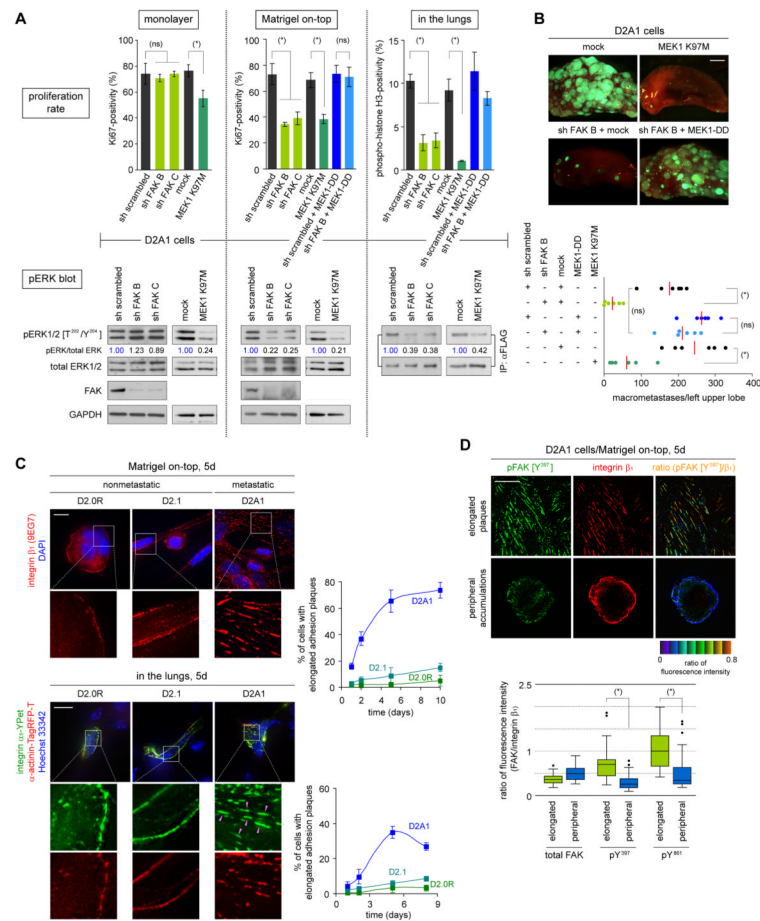
Figure 1. Relationship between adhesion plaque formation, FAK/ERK signaling and proliferation

(A) FAK/ERK signaling and proliferation. Two different shRNA sequences targeting FAK and MEK1 mutants (dominant-negative MEK1 K97M; constitutively active MEK1-DD) were tested for their effects on proliferation and ERK phosphorylation under various conditions. D2A1 cells expressing FLAG-tagged ERK2 (FLAG-ERK) were used to determine ERK phosphorylation levels in cells disseminated to the lungs. Following tail-vein injection, lungs were harvested and lysed, from which FLAG-ERK was immunoprecipitated and analyzed. (ns) $p > 0.5$, (*) $p < 0.02$. In 'pERK blot', values represent the ratio of band intensities relative to that of the control sample.

(B) FAK/ERK signaling and lung colonization. D2A1-GFP cells, in which FAK/ERK signaling was manipulated as indicated, were tail-vein injected into mice. The numbers of macrometastases in the left upper lobe of the lungs (bottom) and representative lobe images (top) are presented. The red bars represent the mean values. MEK1-DD expression restored the proliferation of FAK-knockdown D2A1 cells (see A), allowing them to form abundant macrometastases; this substantiated the role of ERKs as major effectors of FAK in regulating colonization. (ns) $p > 0.5$, (*) $p < 0.001$.

(C) Formation of integrin β_1-containing, elongated adhesion plaques. D2 cells growing in MoT cultures were stained for integrin β_1 (red; with an active-conformation-specific antibody, 9EG7) and nuclei (DAPI: blue) (top-left). D2 cells expressing integrin α_5-YPet (green) and α-actinin-TagRFP-T (red) were tail-vein injected into mice and the distributions of these fluorescent fusion proteins and nuclei (Hoechst 33342; blue) were determined on

lung sections (bottom-left). The presence of elongated adhesion plaques was quantified (right).

(D) FAK phosphorylation levels associated with different integrin β_1-containing structures. MoT-cultured D2A1 cells were dually stained for pFAK (or total FAK) and integrin β_1. Representative images of 'elongated adhesion plaques' and 'peripheral accumulations' with pFAK [Y^{397}] (green)/integrin β_1 (red) staining as well as pseudocolored images representing the ratio of fluorescence intensities are presented (top). The ratio of fluorescence intensities within the region drawn around each of these structures was plotted ($n = 50$; bottom). (*) $p < 1 \times 10^{-9}$.

Bars = 2 mm (B), 10 μm (C,D). Values = means ± SD ($n = 3$; A,C).
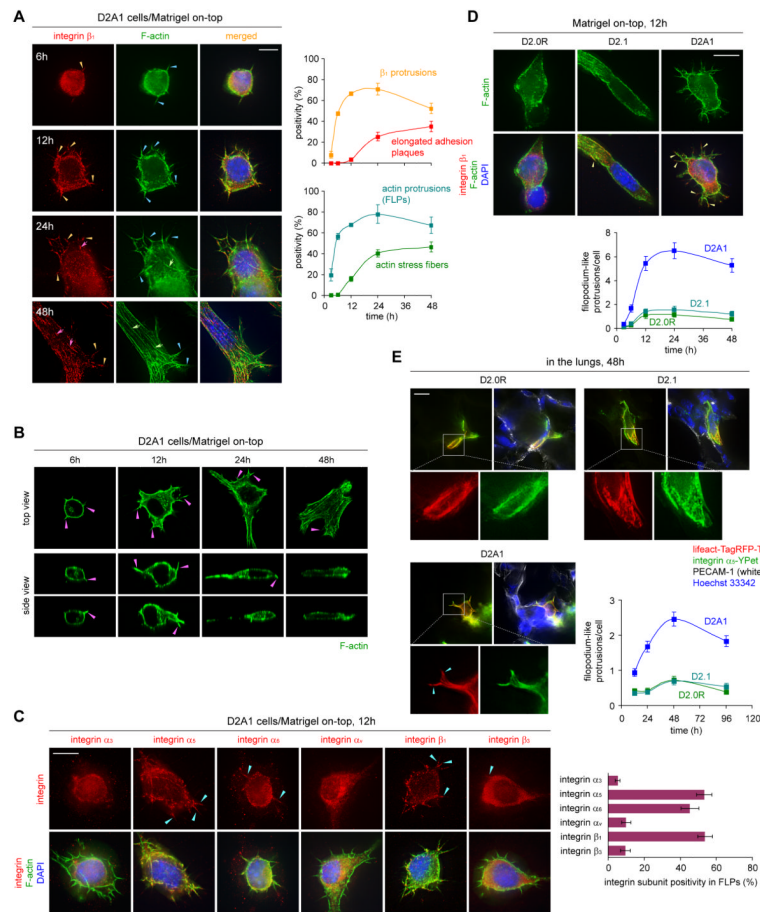
Figure 2. Filopodium-like protrusions that precede adhesion plaque assembly

(**A**) Temporal development of elongated adhesion plaques. The localization of integrin β_1 (red), F-actin (phalloidin; green) and nuclei (blue) was determined at indicated time points in the MoT-cultured D2A1 cells (left). Integrin β_1-containing protrusions (orange arrowheads), elongated adhesion plaques (pink arrows), protrusions of F-actin (blue arrowheads), and actin stress fibers (green arrows) are indicated. The presence of these structures was quantified (right).

(**B**) Upward and downward projections of FLPs. Top and side views of the MoT-cultured D2A1 cells with F-actin-staining (green) are presented with indication of FLPs by the pink arrowheads.

(**C**) Localization of integrin subunits to FLPs. MoT-cultured D2A1 cells were stained for integrin subunits (red), F-actin (green) and nuclei (blue) (left). The accumulation of these subunits to FLPs is indicated (blue arrowheads). The probability with which the length of FLP shaft was covered by the integrin staining was plotted (right).

(**D**) FLP formation in MoT-cultured D2 cells. Integrin β_1-containing FLPs are indicated by the yellow arrowheads (top). The number of FLPs per cell was plotted (bottom).

(**E**) *In vivo* FLP formation. D2 cells expressing lifeact-Tag-RFP-T (red) and integrin α_5-YPet (green) were tail-vein injected into mice. Blood vessels (PECAM-1-staining; white) and nuclei (blue) were visualized together with these fluorescent proteins on lung sections, where FLPs are indicated (blue arrowheads). These cells are not surrounded by the PECAM-1-staining and therefore are likely to have extravasated into the lung parenchyma. The number of FLPs per cell was plotted (bottom-right).

Bars = 10 μm. Values = means ± SD ($n = 3$; A,C) or means ± SEM ($n = 100$; D,E).
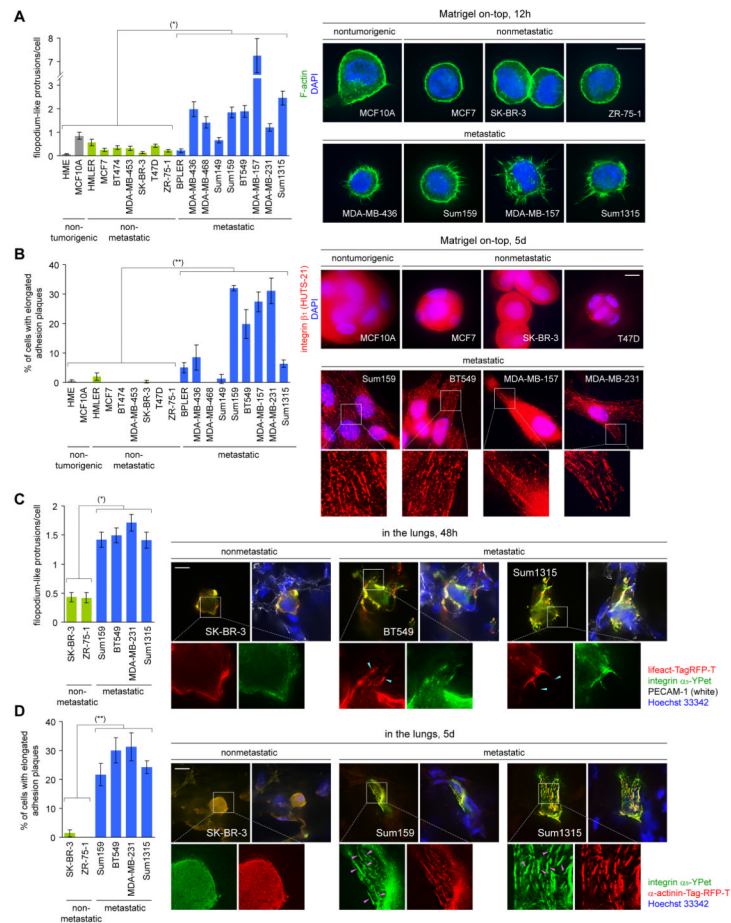
Figure 3. Formation of FLPs and elongated adhesion plaques by various human breast cancer cell lines

(A,B) *In vitro* formation of FLPs and adhesion plaques. Cells were cultured under MoT conditions to quantify the formation of FLPs (A) and elongated adhesion plaques (B). In B, integrin β_1 (red) was stained with an active-conformation-specific antibody, HUTS-21. (*) $p = 0.004$, (**) $p = 0.02$.

(C,D) *In vivo* formation of FLPs and adhesion plaques Cells were engineered to express integrin α_5-YPet (green) and either of lifeact-Tag-RFP-T (red; C) or α-actinin-Tag-RFP-T (red; D). These cells were tail-vein injected into mice to test the formation of FLPs (C) and elongated adhesion plaques (D) within the lung parenchyma. (*) $p = 0.0005$, (**) $p = 0.0008$.

Bars = 10 μm. Values = means $\pm$ SEM ($n = 100$; A,C) or means $\pm$ SD ($n = 3$; B,D).
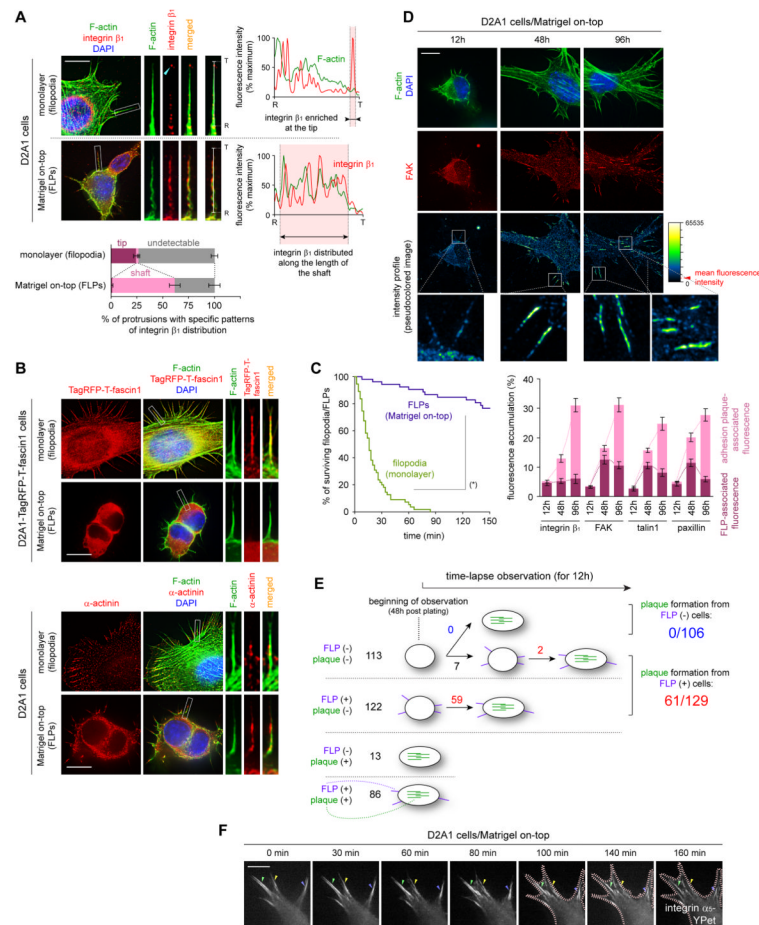
Figure 4. FLP formation as a prerequisite for adhesion plaque assembly

(A–C) Comparison of filopodia (monolayer) and FLPs (MoT). Cells growing in either monolayer or MoT culture were stained for F-actin (green; A,B), integrin β_1 (red; A) and α-actinin (red; B, bottom). Fascin1 localization was determined by the use of TagRFP-T-fascin1 fusion protein (red; B, top). In A, the fluorescence intensity along the line (root [R] – tip [T]) was plotted (right) and integrin β_1 distribution within each protrusion types was scored (bottom). In B, fascin1 was localized along the length of filopodia but not to FLPs; α-actinin was detected at the root of filopodia and along the length of FLPs. In C, the kinetics of the assembly and disassembly of these protrusions are represented by the Kaplan-Meier survival curves. D2A1 cells expressing the lifeact-YPet actin marker were analyzed by time-lapse microscopy. (*) $p < 0.0001$ (by log-rank test).

(D) Initial accumulation of adhesion plaque proteins to FLPs. The localization of F-actin (green), nuclei (blue) and FAK (red) was determined at indicated time points (top). The pseudocolored images represent the profiles of FAK-staining intensity. The accumulation of integrin β_1 and various adhesion plaque proteins to FLPs and elongated adhesion plaques was scored (bottom).

(E,F) Functional connection between FLPs and elongated adhesion plaques. Integrin α_5-YPet-expressing D2A1 cells growing under the MoT conditions were analyzed by time-lapse microscopy. In E, cells were classified by the presence or absence of FLPs (purple) and elongated adhesion plaques (green) at the beginning of observation. Initially-adhesion-plaque-negative cells (113 + 122 cells) were analyzed for the subsequent development of FLPs and elongated adhesion plaques. In F, an example of progressive inward movement of

FLP-associated integrin α_5-YPet clumps (arrowheads; 0–80 min) and subsequent outward extension of the plasma membrane, which cooperatively converted these integrin clumps into the ones constituting elongated adhesion plaques (arrowheads; 140–160 min), is presented. The pink dotted lines represent cell edges.

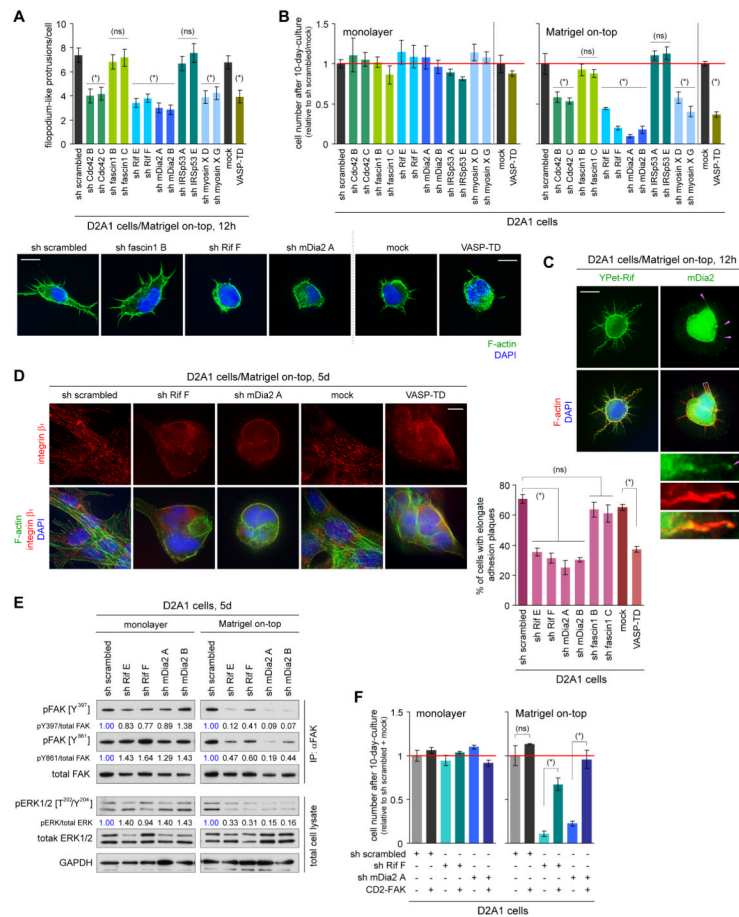Bars = 10 μm. Values = means ± SD ($n = 3$; A) or means ± SEM ($n = 30$; D).

Figure 5. Identification of the molecular regulators of FLP formation

(A,B) Screening of filopodium regulators for their involvement in FLP formation and proliferation. D2A1 cells, manipulated to block the expression or function of filopodium-associated proteins, were tested for FLP formation under MoT culture conditions (A). Two different shRNA sequences were tested for each knockdown targets. The effects of these manipulations on the cell number after 10 days of monolayer or MoT cultures were also tested (B). (ns) $p > 0.2$, (*) $p < 0.02$ (vs control).

(C) Localization of Rif and mDia2 to FLPs. YPet-Rif fusion protein was used for analyzing Rif distribution, whereas mDia2 localization was determined by direct immunostaining (green; mDia2 localization at FLP tips is indicated by pink arrowheads). F-actin (red) and nuclei (blue) were also visualized.

(D) Role of Rif/mDia2 signaling and Ena/VASP proteins in adhesion plaque formation. Some of the engineered D2A1 cells described in A were cultured under MoT conditions. The presence of integrin β_1-containing, elongated adhesion plaques was quantified (right). (ns) $p > 0.05$, (*) $p < 0.0005$.

(E) Role of Rif/mDia2 signaling in FAK/ERK activation. Lysates from the indicated cell types were immunoprecipitated with an anti-total FAK antibody and analyzed for FAK phosphorylation levels. These lysates were also analyzed by direct immunoblotting for ERK phosphorylation levels.

(F) Rescue of proliferation defects by CD2-FAK expression. The control, Rif-knockdown and mDia2-knockdown D2A1 cells were further engineered to express the constitutively active CD2-FAK fusion protein. Cell numbers after 10-day-culture were plotted. (ns) $p > 0.1$, (*) $p < 0.005$.

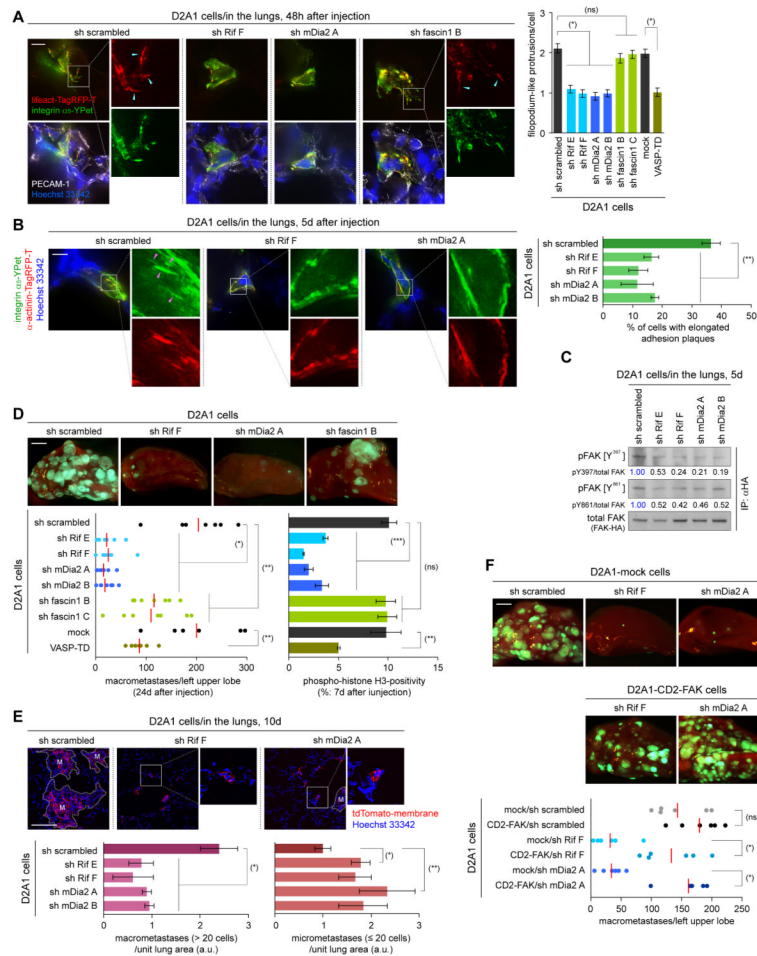Bars = 10 µm. Values = means ± SEM (n = 100; A) or means ± SD (n = 3; B,D,F).

Figure 6. Rif/mDia2 signaling and lung colonization

(A,B) Rif/mDia2 signaling and *in vivo* formation of FLPs and elongated adhesion plaques. D2A1 cells expressing integrin α_5-YPet (green) and either of lifeact-Tag-RFP-T (red; A) or α-actinin-Tag-RFP-T (red; B) were further engineered as indicated and tested for the formation of FLPs (blue arrowheads; A) and elongated adhesion plaques (pink arrowheads; B) within the lung parenchyma. The number of FLPs per cell (A, right) and the presence of elongated adhesion plaques (B, right) were quantified (right). (ns) $p > 0.1$, (*) $p < 1 \times 10^{-8}$, (**) $p < 0.01$.

(C) Rif/mDia2 signaling and *in vivo* FAK activation. D2A1 cells expressing HA-tagged FAK (FAK-HA), with or without Rif- or mDia2-knockdown, were tail-vein injected into mice. Lysates were prepared from the lungs, from which FAK-HA was immunoprecipitated and analyzed.

(D,E) Rif/mDia2 signaling and lung colonization following tail-vein injection. In D, the D2A1-GFP cells, engineered as in A, were tested for macrometastasis formation and proliferation in the lungs. (ns) $p > 0.5$, (*) $p < 0.0002$, (**) $p < 0.05$, (***) $p < 0.005$. In E, lung sections were prepared 10 days after the injection of the engineered D2A1 cells, also expressing membrane-targeted tdTomato (tdTomato-membrane). The numbers of macroscopic (> 20 cells/colony) and microscopic (20 cells/colony) metastases were plotted (bottom). 'M'-labeled regions indicate macrometastases. (*) $p < 0.02$, (**) $p < 0.05$.

(F) Restoring metastasis-forming ability by CD2-FAK expression. The effects of CD2-FAK expression on the number of lung macrometastases formed by the control, Rif-knockdown

and mDia2-knockdown D2A1 cells following tail-vein injection were tested. (ns) $p > 0.1$, (*) $p < 0,005$.

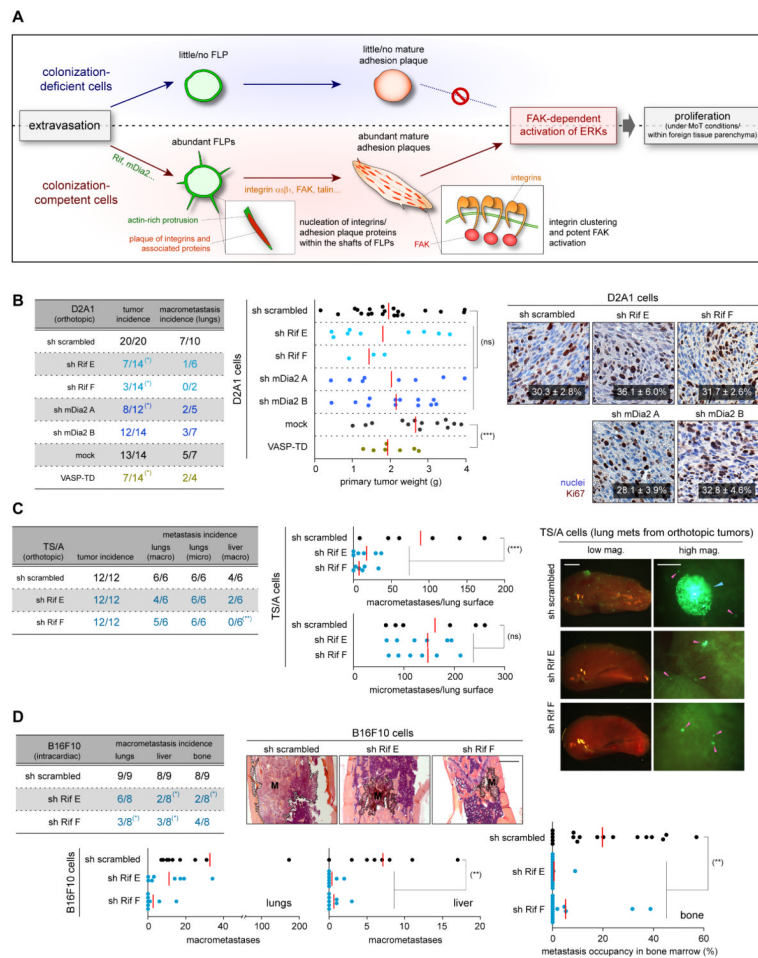Bars = 10 µm (A,B), 2 mm (D,F), 0.1 mm (E). Values = means ± SEM ($n = 150$; A) or means ± SD ($n = 3$; B,D,E).

Figure 7. Rif/mDia2 signaling in primary tumor formation and spontaneous metastasis
(**A**) Cell-biological and associated signaling events critical to the initial proliferation of cancer cells within foreign tissue parenchyma.
(**B,C**) Role of FLP-regulating proteins in primary tumor formation and spontaneous metastasis. The D2A1-GFP cells (B) and TS/A-GFP cells (C), each engineered as indicated, were implanted into mouse mammary fat pads. Subsequent formation of primary tumors and the incidences of spontaneous metastases in the lungs and liver were analyzed. In B, Ki67-staining positivity was scored on the primary tumor sections (right). Values = means ± SD ($n = 3$). In C, a macrometastasis and micrometastases were indicated by blue and pink arrowheads, respectively, on the representative lung images (right). (*) $p < 0.04$, (**) $p = 0.03$ (vs control) by Fisher's exact test. (ns) $p > 0.2$, (***) $p < 0.05$ by Student's t-test.
(**D**) Role of Rif in metastasis formation by the intracardially-injected B16F10 cells. The control and Rif-knockdown-B16F10 cells were intracardially injected into mice. Metastasis formation in the lungs, liver and bone marrow was analyzed. (*) $p < 0.05$ (vs sh scrambled) by Fisher's exact test. (**) $p < 0.02$ by Student's t-test.
Bars = 0.1 mm (B), 2 mm (C [low mag.], D), 0.5 mm (C [high mag.]).